

# Charge Exchange Reactions and Applications to Nuclear- Astrophysics

Myung-Ki Cheoun

*Soongsil University, Seoul, Korea*

*K. S. Kim, E. Ha, C. Ryu...*

*G. Mathews,*

*T. Kajino, T. Hayakawa, T. Maruyama ...*

*F. Simkovic, A. Faessler...*

# Contents

## 0. Introduction

## 1. Charge exchange reactions within the QRPA

### 1-1. Beta decays, (n,p) and (p,n) reactions

### 1-2. Neutrino reactions by CC and NC

### 1-3. Deformed QRPA

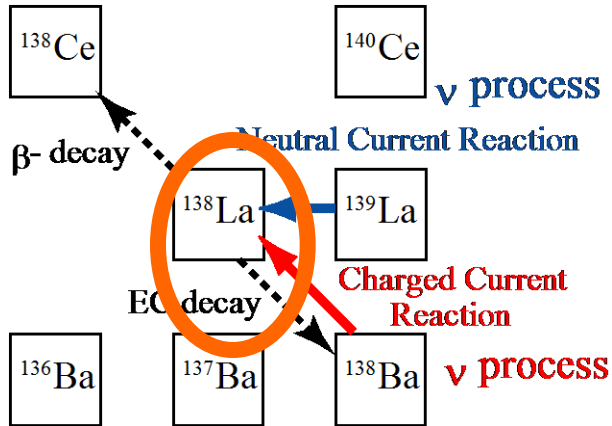
## 2. Applications to Nuclear astrophysics

### 2-1. Neutrino reactions on $^{12}\text{C}$ and $^{56}\text{Fe}$

### 2-2. Neutrino-process for proton nuclei ( $^{138}\text{La}$ , $^{180}\text{Ta}$ , $^{92}\text{Nb}$ , $^{98}\text{Tc}$ )

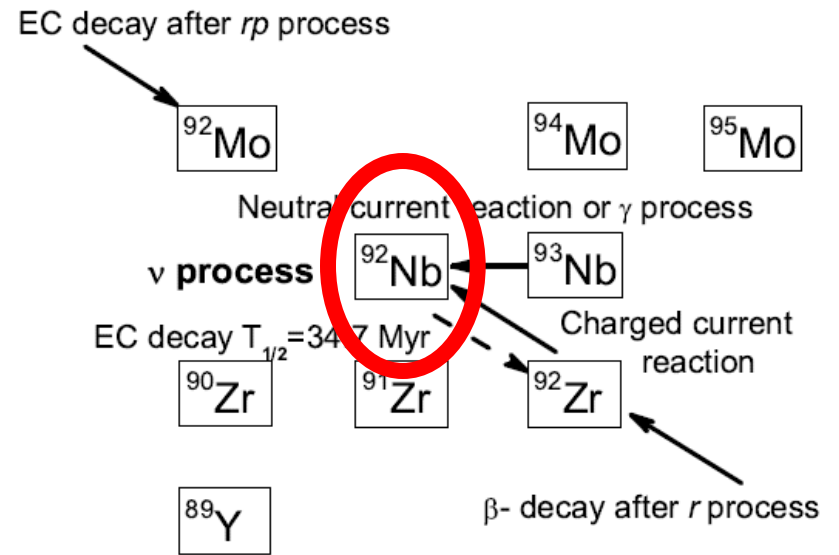
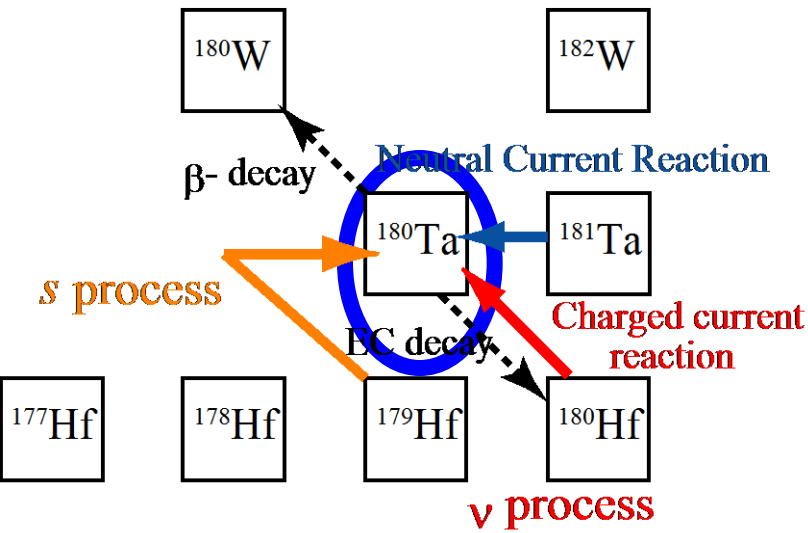
### 2-3. Neutrino reactions on $^{40}\text{Ar}$ for ICARUS

## 3. Summary and Future works



Isotopic ratios:

$^{92}\text{Nb}/^{93}\text{Nb}$	$\gg$	Solar: $10^{-3} - 10^{-5}$
$^{138}\text{La}/^{139}\text{La}$	$>$	0.001
$^{180}\text{Ta}/^{181}\text{Ta}$	$>$	0.0001



# Motivation

# Neutrino Energy

Cross Section

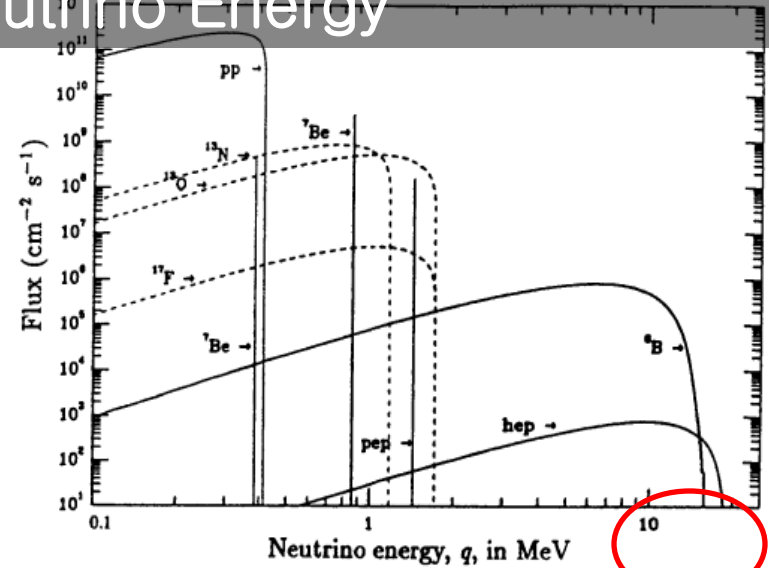
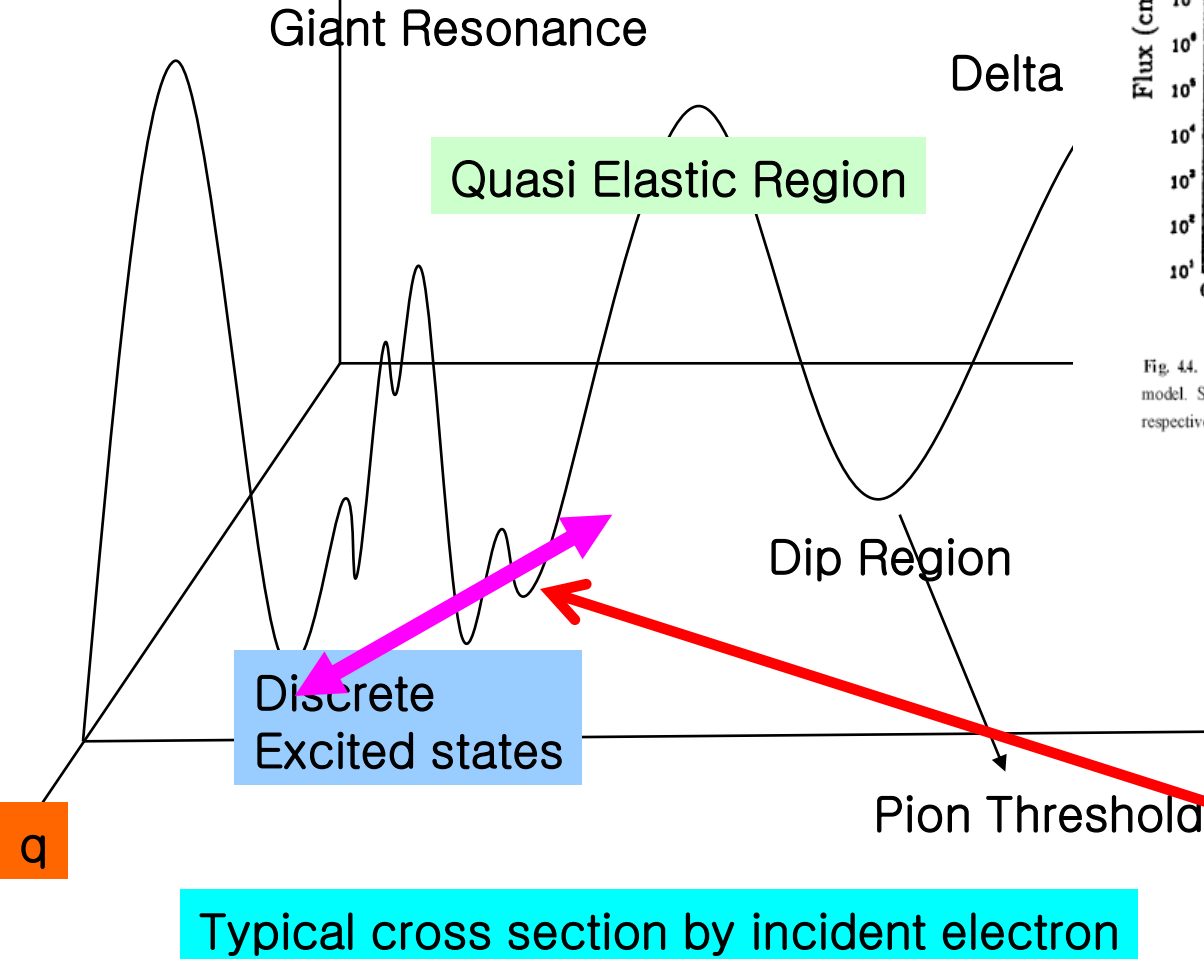
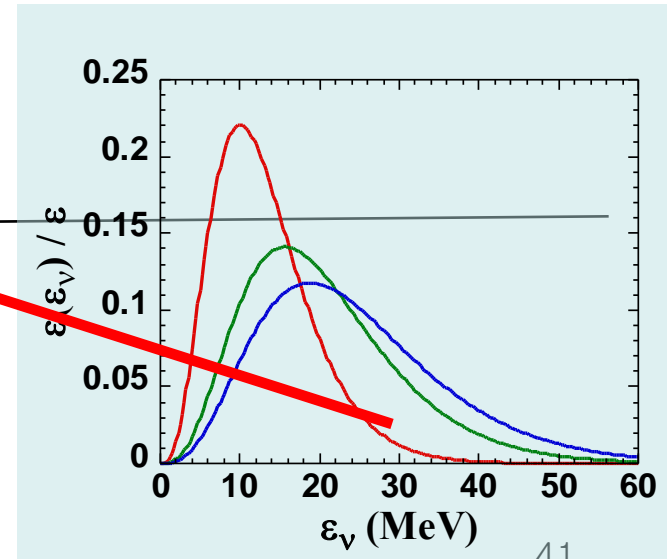
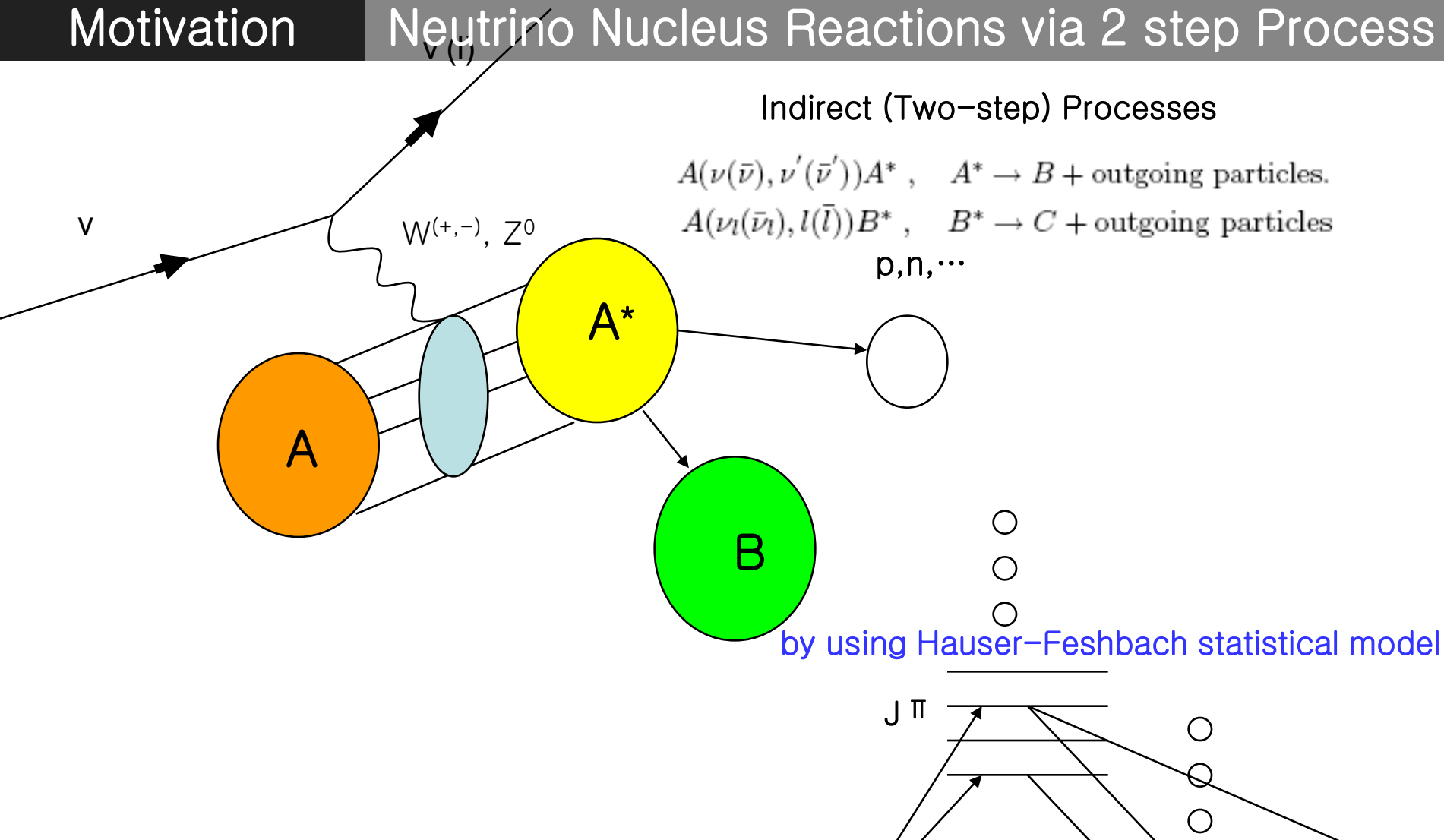


Fig. 44. Solar neutrino spectrum. Energy spectrum of solar neutrinos, as predicted by the standard solar model. Solid and dashed curves distinguish between neutrinos produced in the pp-chains and the CNO cycle, respectively. (From 49.)



$$T(\nu_e) = 3.2 \text{ MeV} < T(\bar{\nu}_e) = 5.0 \text{ MeV} < T(\nu_{\mu,\tau}) = T(\bar{\nu}_{\mu,\tau}) = 6.0 \text{ MeV}$$



How to describe the ground and excited states  
And decays with particle emissions ?

# Pairing of Like and Unlike nucleons

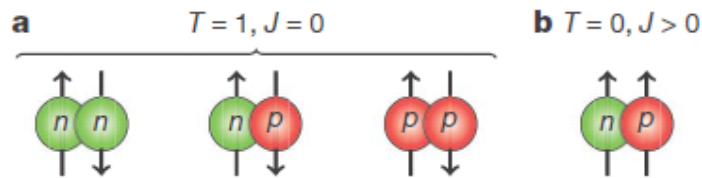


Figure 1 | Schematic illustration of the two possible pairing schemes in nuclei. a, The normal isospin  $T = 1$  triplet. The two like-particle pairing components are responsible for most known effects of nuclear superfluidity. Within a given shell these isovector components are restricted to spin zero owing to the Pauli principle. b, Isoscalar  $T = 0$  neutron-proton pairing. Here the Pauli principle allows only non-zero components of angular momentum.

- neutron-neutron, proton-proton ( $T = 1$ )
- neutron-proton ( $T = 1$  and  $0$ ) couples  $J = L - 1$  and  $J = L + 1$  by tensor force. For example,  ${}^3S_1$  and  ${}^3D_1$  states play roles
- The np pairing is vital for the exotic nuclei in the nucleo-synthesis with the deformations

- (iii) *Nucleon-nucleon interaction.* In the  $0\nu\beta\beta$ -decay calculations both schematic zero-range [40] and realistic interactions were considered. In Ref. [41]  $G$ -matrix of the Paris potential approximated by a sum of Yukawa terms was used. The interaction employed by the Tuebingen group has been the Brueckner  $G$  matrix that is a solution of the Bethe-Goldstone equation with Bonn (Bonn CD, Argonne, Nijmegen) one boson exchange potential. The results do not depend significantly on the choice of the NN interaction [19].



In Nucleus

$$G_{ab,cd} = \bar{v}_{ab,cd} + \frac{1}{2} \sum_{m,n} \bar{v}_{ab,mm} \frac{1}{E - \epsilon_m - \epsilon_n + i\eta} G_{mm,cd}$$
$$\rightarrow G = \bar{v} + \bar{v} \frac{Q_A}{E - H_0} G$$

Bethe-Goldstone Eq.

$$\rightarrow G = \frac{\bar{v}}{1 - \bar{v} Q_A / (E - H_0)}$$

$Q_A = \sum_{(m,n) > \epsilon_F} |mm\rangle \langle mm|$   
 $H_0 = \text{Hamiltonian in shell index model}$

→ Even if  $\bar{v}$  is infinite,  $G$  is finite

$$\begin{aligned}
\left(\frac{d\sigma_\nu}{d\Omega}\right)_{(\nu/\bar{\nu})} &= \frac{G_F^2 \epsilon k}{\pi (2J_i + 1)} \left[ \sum_{J=0} (1 + \vec{\nu} \cdot \vec{\beta}) | \langle J_f || \hat{\mathcal{M}}_J || J_i \rangle |^2 \right. \\
&+ (1 - \vec{\nu} \cdot \vec{\beta} + 2(\hat{\nu} \cdot \hat{q})(\hat{q} \cdot \vec{\beta})) | \langle J_f || \hat{\mathcal{L}}_J || J_i \rangle |^2 - \\
&\hat{q} \cdot (\hat{\nu} + \vec{\beta}) 2 \operatorname{Re} \langle J_f || \hat{\mathcal{L}}_J || J_i \rangle \langle J_f || \hat{\mathcal{M}}_J || J_i \rangle^* \\
&+ \sum_{J=1} (1 - (\hat{\nu} \cdot \hat{q})(\hat{q} \cdot \vec{\beta})) (| \langle J_f || \hat{\mathcal{T}}_J^{el} || J_i \rangle |^2 + | \langle J_f || \hat{\mathcal{T}}_J^{mag} || J_i \rangle |^2) \\
&\left. \pm \sum \hat{q} \cdot (\hat{\nu} - \vec{\beta}) 2 \operatorname{Re} [ \langle J_f || \hat{\mathcal{T}}_J^{mag} || J_i \rangle \langle J_f || \hat{\mathcal{T}}_J^{el} || J_i \rangle^* ] \right],
\end{aligned}$$

$$\sigma(E_\nu) = \frac{G_F^2 \cos^2 \theta_c}{\pi \hbar^4 c^3} \sum_i k_i \epsilon_i F(Z, \epsilon_i) [B_i(GT) + B_i(F)], \quad (8)$$

where  $k_i$  and  $\epsilon_i$  refer to the momentum and total energy of the outgoing electron and  $F(Z, \epsilon_i)$

$$R_{CL}(\mathbf{q}, \omega) = \sum_{J=0} | \langle J_f || \hat{\mathcal{M}}_J(\mathbf{q}) + \frac{\omega}{q} \hat{\mathcal{L}}_J(\mathbf{q}) || J_i \rangle |^2,$$

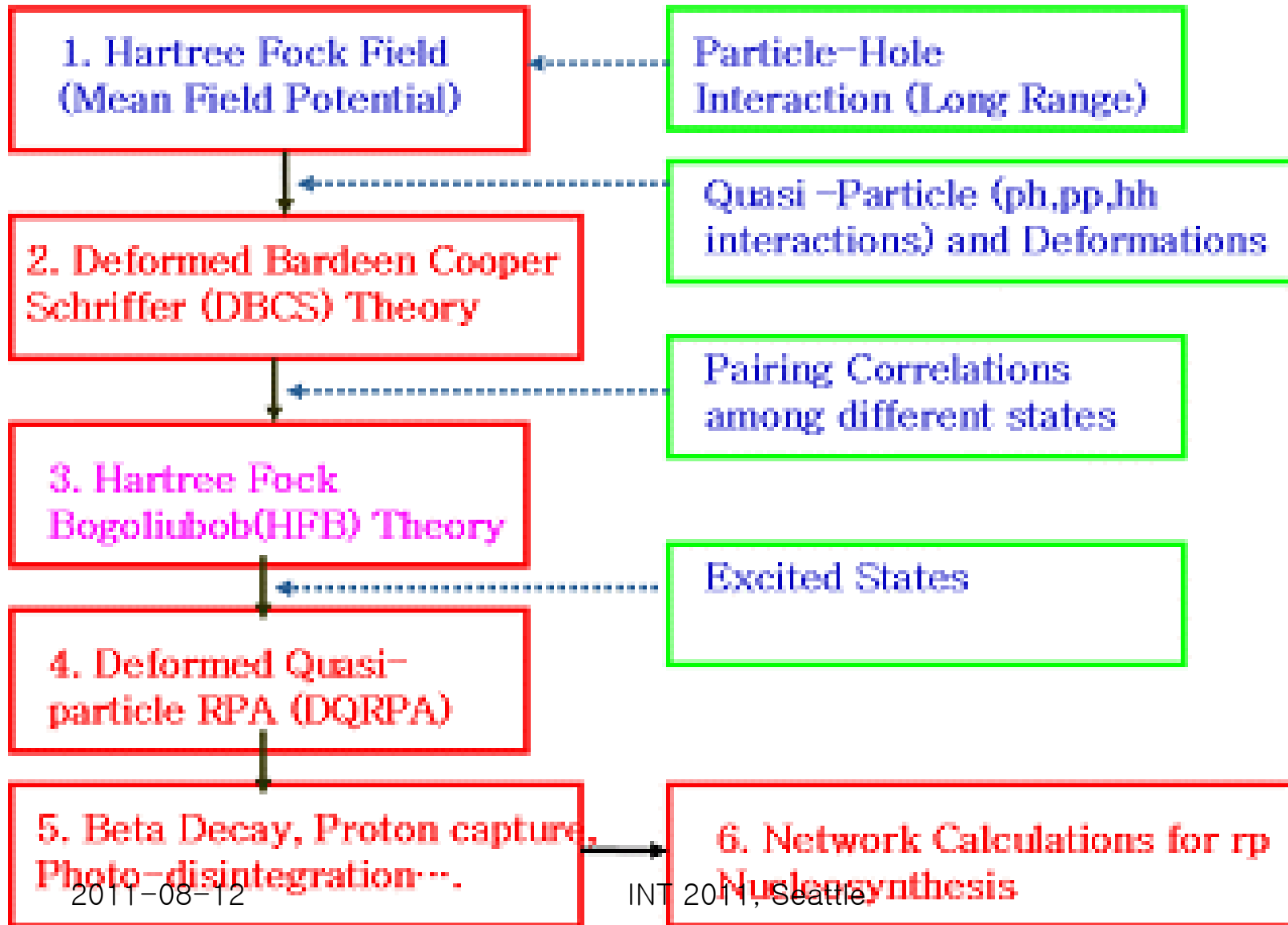
$$R_T(\mathbf{q}, \omega) = \sum_{J=0} | \langle J_f || \hat{\mathcal{T}}_J^{el}(\mathbf{q}) || J_i \rangle |^2 + | \langle J_f || \hat{\mathcal{T}}_J^{mag}(\mathbf{q}) || J_i \rangle |^2,$$

$$R_I(\mathbf{q}, \omega) = \sum_{J=0} 2 \operatorname{Re} \langle J_f || \hat{\mathcal{T}}_J^{el}(\mathbf{q}) || J_i \rangle \langle J_f || \hat{\mathcal{T}}_J^{mag}(\mathbf{q}) || J_i \rangle,$$

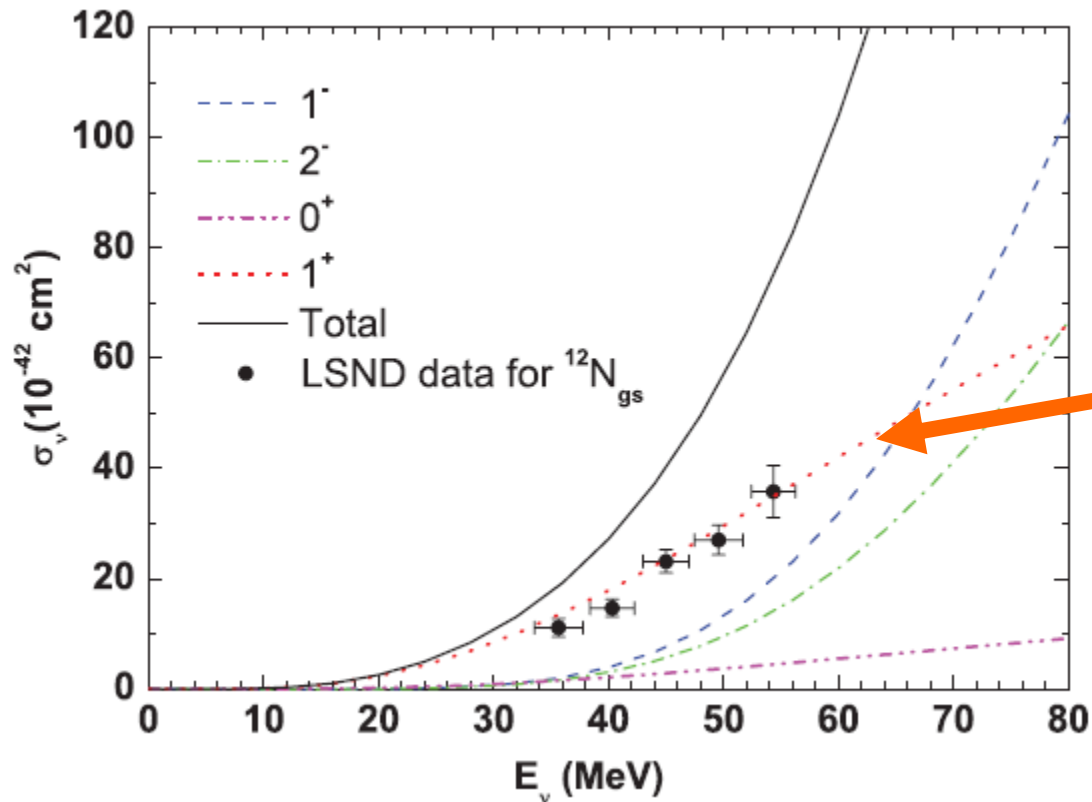
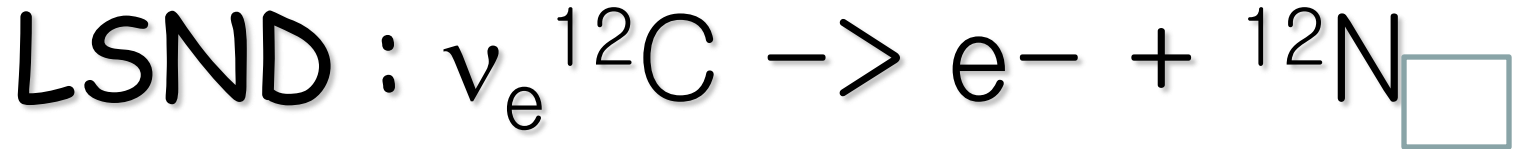
$$\left(\frac{d\sigma_\nu}{dq^2}\right)_{\nu/\bar{\nu}} = \frac{2G_F^2 \epsilon \cos^2(\frac{\theta}{2})}{\nu 2(J_i + 1)} \left[ R_{CL}(\mathbf{q}, \omega) + C(\theta, \mathbf{q}) R_T(\mathbf{q}, \omega) \mp \tan(\frac{\theta}{2}) C(\theta, \mathbf{q}) R_I(\mathbf{q}, \omega) \right]$$



# FLOW of Computer Program



Results :  
Neutrino Reactions  
for  $^{12}\text{C}$ ,  $^{56}\text{Fe}$ ,  $^{92}\text{Nb}$ ,  $^{138}\text{La}$  and  
 $^{180}\text{Ta}$ ,  $^{40}\text{Ar}$ .



O.K. !!

PHYSICAL REVIEW C **81**, 028501 (2010)

Neutrino reactions on  ${}^{12}\text{C}$  by the quasiparticle random-phase approximation (QRPA)

Myung-Ki Cheoun,<sup>1,4,\*</sup> Eunja Ha,<sup>1</sup> Su Youn Lee,<sup>1</sup> K. S. Kim,<sup>2</sup> W. Y. So,<sup>3</sup> and Toshitaka Kajino<sup>4,5</sup>

**Table 1.** Comparison of calculated and measured flux averaged cross sections for the  $\nu$ - $^{12}\text{C}$  reaction in units of  $10^{-42} \text{ cm}^2$ , and half life time of neighboring nuclei. The cross sections are folded by the corresponding DAR neutrino spectra, where the Michel spectrum is used for the energies  $\nu_e$  and  $\nu_\mu$  is fixed at 29.8 MeV. 'K' and 'L' mean Karmen and LSND groups results, respectively. Shell model (SM) and continuum RPA (CRPA) results are cited from [3] and [9], respectively. (9.834\*) is a result with no Coulomb correction.

	$^{12}\text{C}(\nu_e, e^-)^{12}\text{N}_{g.s.}$	$^{12}\text{C}(\nu_e, e^-)^{12}\text{N}^*$	$\beta^{(-)} : (^{12}\text{B}(1^+) \rightarrow ^{12}\text{C})$
Experimental data	$8.9 \pm 0.3 \pm 0.9$ [12]'L' $9.1 \pm 0.5 \pm 0.8$ [13]'K'	$4.3 \pm 0.4 \pm 0.6$ [12]'L' $5.1 \pm 0.5 \pm 0.5$ [14]'K'	23.6 ms
Ours	11.53 (9.834*)	6.1	21.33 ms
SM	9.06–8.48	5.22–4.87	
CRPA	8.9	5.4	
	$^{12}\text{C}[(\nu_e, \nu'_e) + (\bar{\nu}_\mu, \bar{\nu}'_\mu)]^{12}\text{N}_{g.s.}$	$^{12}\text{C}[(\nu_\mu, \nu'_\mu)]^{12}\text{C}^*$	$\beta^{(+)}(EC) : (^{12}\text{N}(1^+) \rightarrow ^{12}\text{C})$
Experimental data	$10.4 \pm 1.0 \pm 0.9$ [13]'K'	$3.2 \pm 0.5 \pm 0.4$ [15]'K'	11.0 ms
Ours	9.92	3.60	10.34 ms
SM	9.76–8.27	2.68–2.26	
CRPA	10.5		

Cross sections averaged by incident neutrino flux  $\langle \sigma \rangle = \int dE_\nu f(E_\nu) \sigma(E_\nu) / \int dE_\nu f(E_\nu)$  for exclusive and inclusive reactions via charged and neutral currents are tabulated

Flux averaged C.S. for DAR

N. PAAR, D. VRETENAR, T. MARKETIN, AND P. RING

PHYSICAL REVIEW C 77, 024608 (2008)

TABLE II. Flux-averaged cross sections for the  $\nu_e$  reaction on  $^{16}\text{O}$ ,  $^{56}\text{Fe}$ , and  $^{208}\text{Pb}$  target nuclei.

	$^{16}\text{O}(\nu_e, e^-)^{16}\text{F}$ $\langle\sigma\rangle(10^{-42} \text{ cm}^2)$	$^{56}\text{Fe}(\nu_e, e^-)^{56}\text{Co}$ $\langle\sigma\rangle(10^{-42} \text{ cm}^2)$	$^{208}\text{Pb}(\nu_e, e^-)^{208}\text{Bi}$ $\langle\sigma\rangle(10^{-42} \text{ cm}^2)$
SM ( $0\hbar\omega \times 0.64$ ) [62]	10.8		
TM [65]		214	
TDA (SKIII) [66]			2954,3204
RPA [64]	14.55	277	2643
CRPA (WS+LM) [67]		240	3620
(Q)RPA (SIII,SGII)	16.90,17.20 [21]	352 [63]	4439 [23]
PN-RQRPA (DD-ME2)	13.18	140	2789
Exp. (KARMEN) [9,67]		$256 \pm 108 \pm 43$	

Our results : 1.418 (-40) : Fermi Coulomb Correction

With np pairing 1.735 (-40) !!!!



O.K. !!



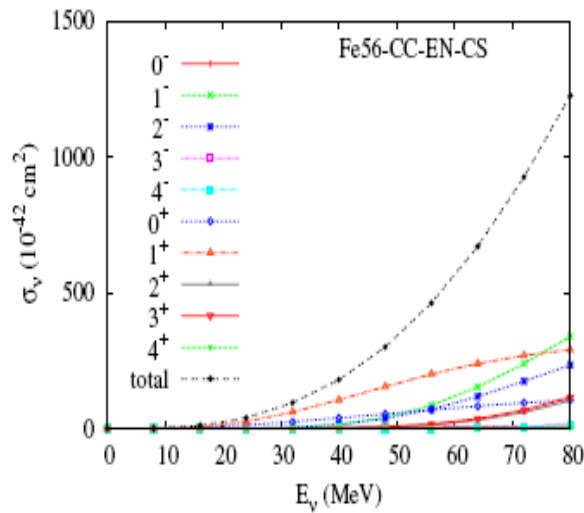
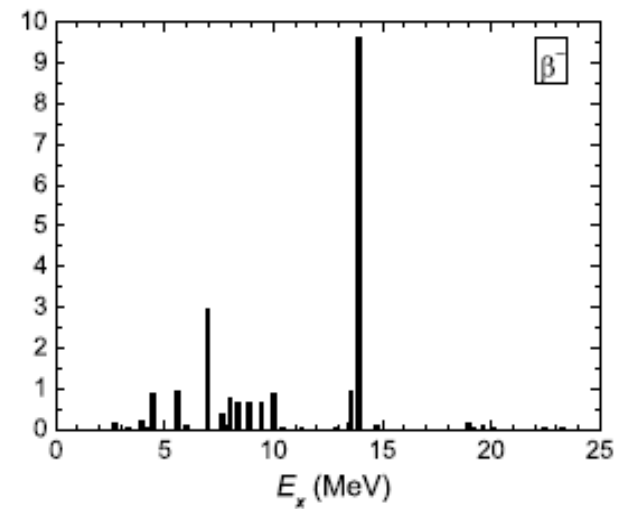
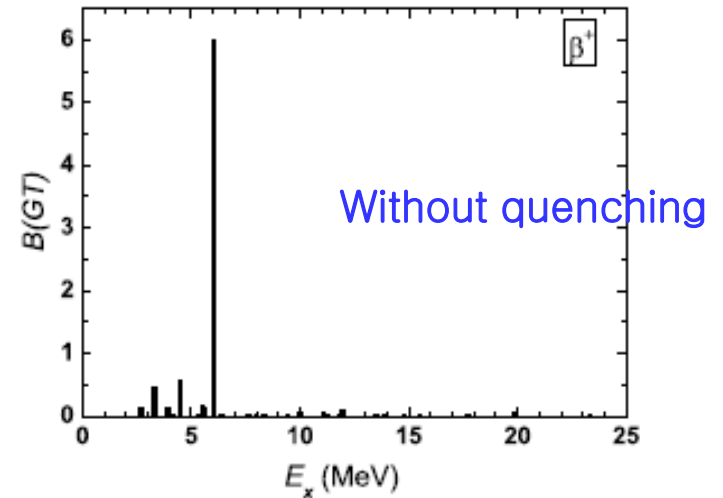


Figure 6. Cross sections of the  $^{56}\text{Fe}(\nu_e, e^-)^{56}\text{Co}^*$  reaction for  $J_\pi = 0^\pm-4^\pm$  states. Each multipole state contribution and total sum are presented.



We need the quenching for the exp. data.

Since results of the total GT strength are also reported in [40], we take the summation of the distributions. Our results for the total GT strength with a universal quenching factor  $f_q^2 = (0.74)^2$  [6, 40] are 11.38 and 4.41 for  $B(GT_\mp)$ , respectively. They are consistent with those of experimental data,  $9.9 \pm 2.4$  [39] and  $2.8 \pm 0.3$  [40], respectively. As shown in

$^{138}\text{Ba}(^3\text{He}, t)^{138}\text{La}$  reaction

PRL 98, 082501 (2007) PHYSICAL REV

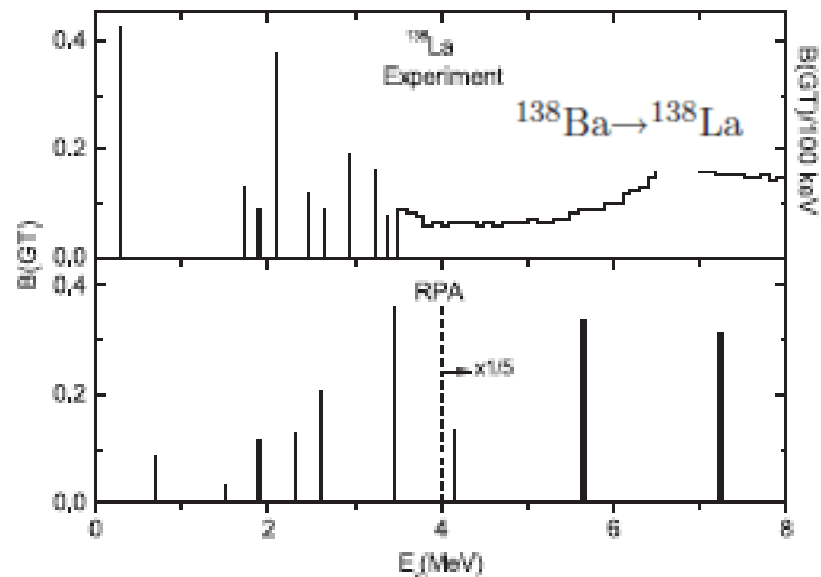
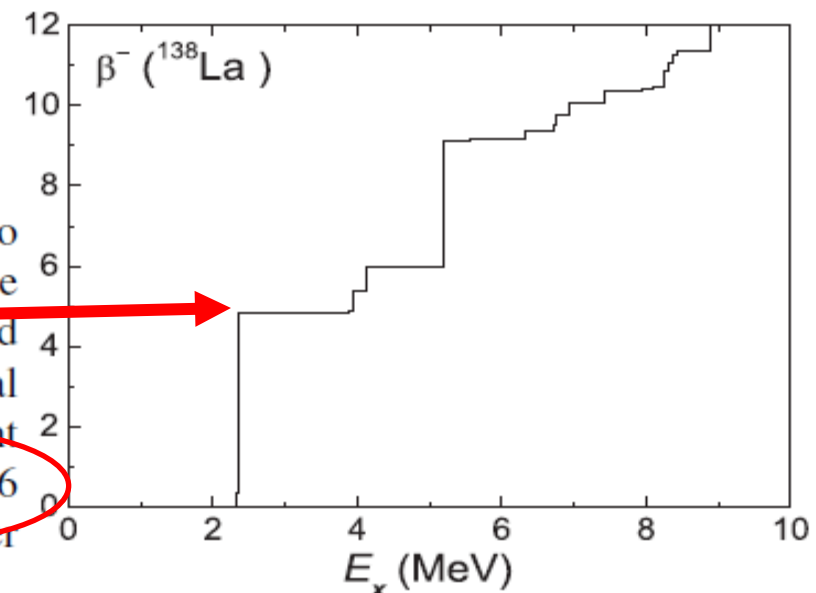
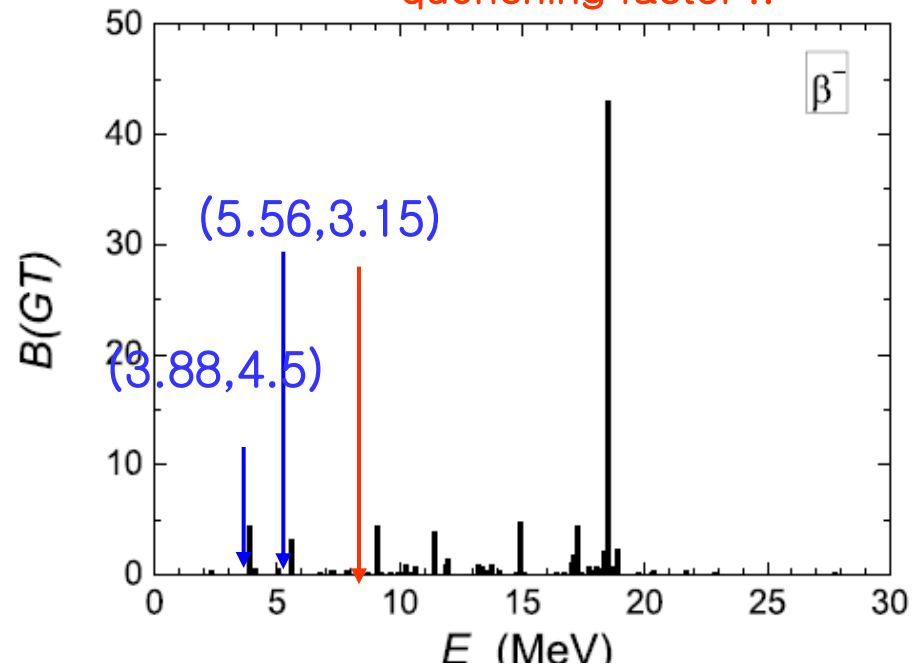
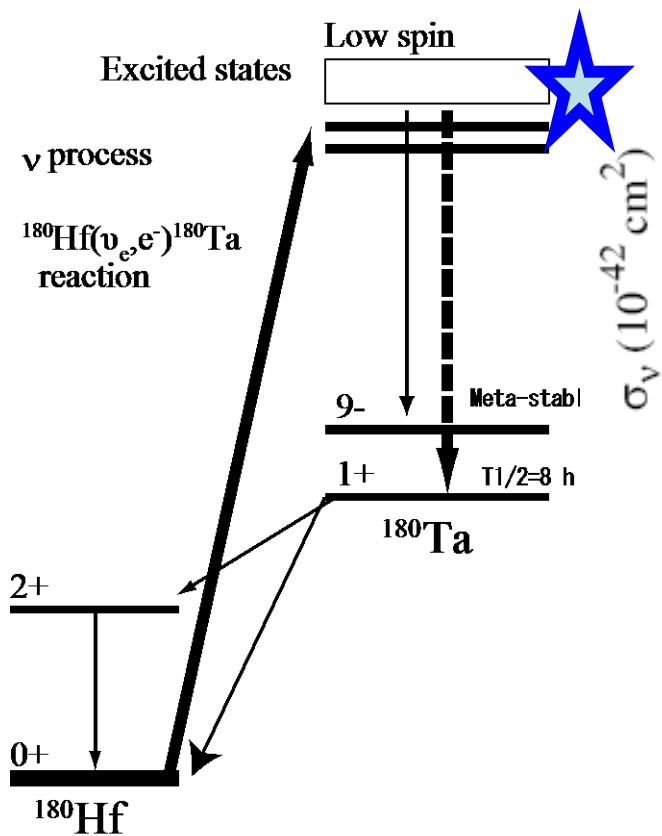


FIG. 3. GT strength distribution in  $^{138}\text{La}$ . Top: present work. Bottom: RPA calculation used in Ref. [2].

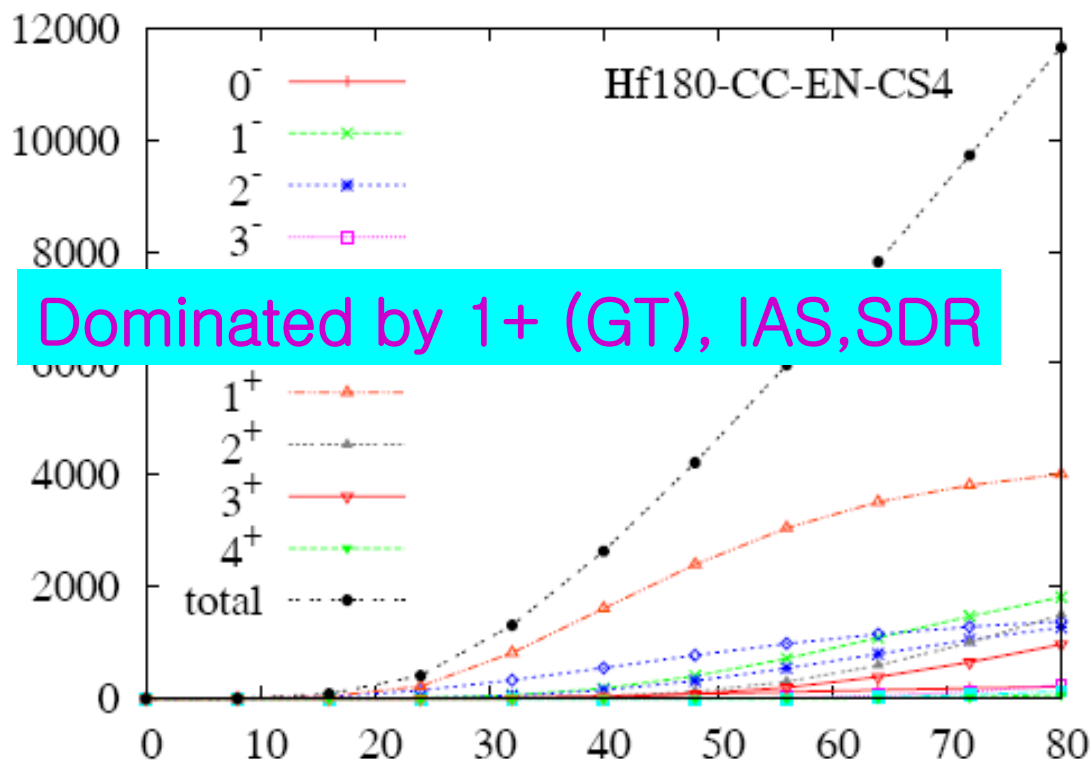
We reproduce experimental (GT) strength distribution by the quenching factor !!



Running sums of the GT(-) strength distribution up to 10 MeV are shown in the right panels. Our results for the running sum up to 8 MeV are 5.5 and 3.8 for  $^{138}\text{La}$  and  $^{180}\text{Ta}$ , respectively, if we take into account the universal quenching factor  $f_q = 0.74$  for the axial coupling constant  $g_A$ . They reproduce well the experimental data,  $5.8 \pm 1.6$  and  $4.4 \pm 0.9$ , respectively, reported in Ref. [12]. For other

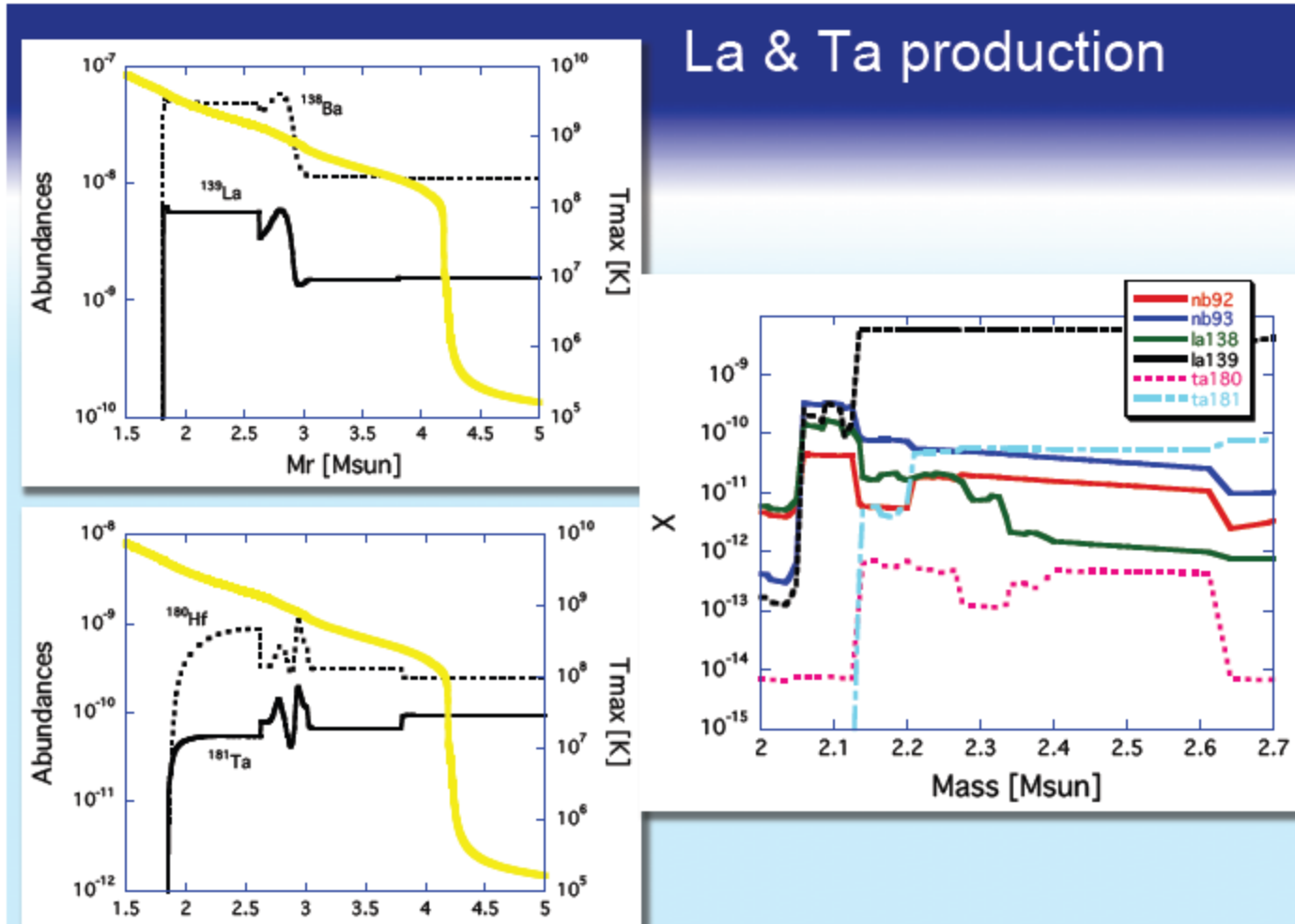


$$\langle \sigma_\nu \rangle = \frac{\int dE_\nu \sigma_\nu(E_\nu) f(E_\nu)}{\int dE_\nu f(E_\nu)},$$



T(MeV)	$^{138}\text{La}$			$^{180}\text{Ta}$		
	Exp.	RPA	Ours	Exp.	RPA	Ours
4	74	61	68	151	115	76
6	226	156	254	399	272	316
8	435	281	554	752	485	672

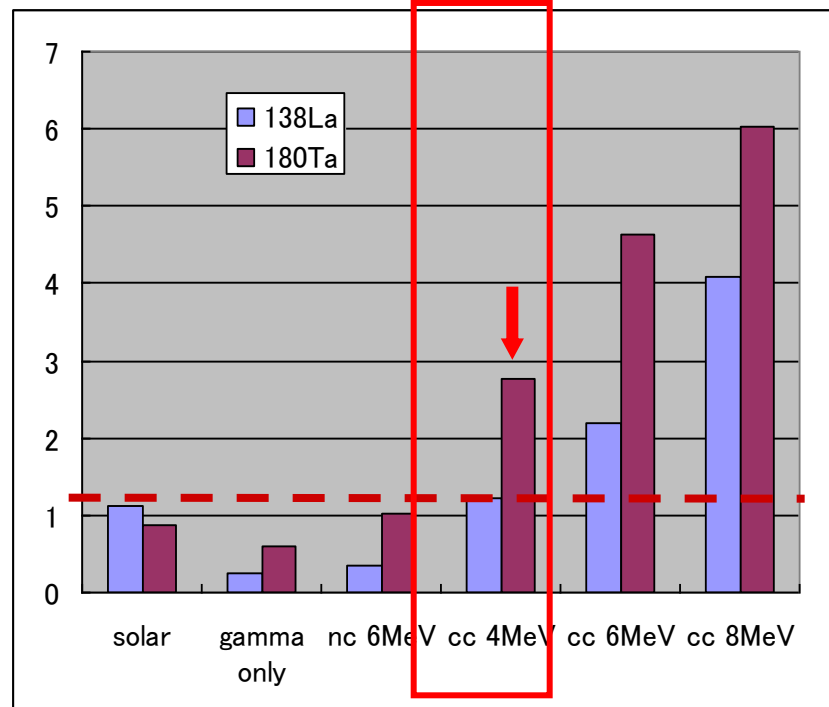
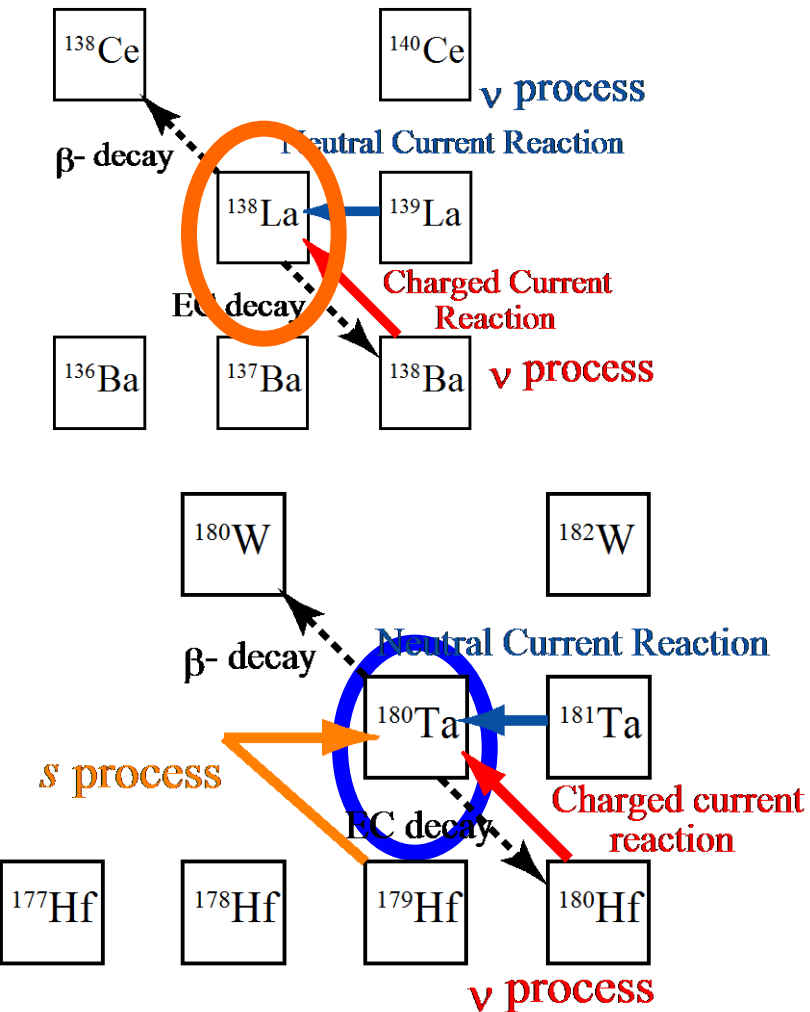




PHYSICAL REVIEW C 82, 035504 (2010)

Neutrino reactions on  $^{138}\text{La}$  and  $^{180}\text{Ta}$  via charged and neutral currents by the quasiparticle random-phase approximation

Myung-Ki Cheoun,<sup>1,\*</sup> Eunja Ha,<sup>1</sup> T. Hayakawa,<sup>2</sup> Toshitaka Kajino,<sup>3,4</sup> and Satoshi Chiba<sup>5</sup>



Hayakawa et.al, (2010)

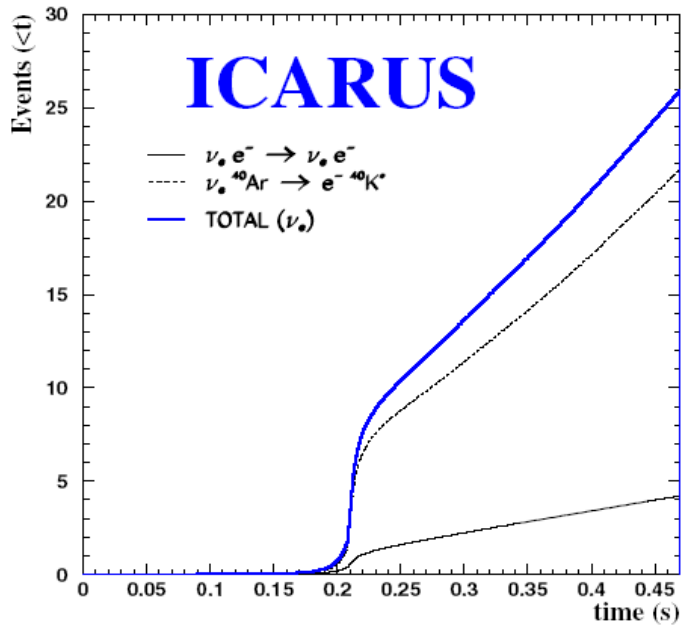


Figure 11. Integrated number of  $\nu_e$  events as a function of time for the elastic and absorption channels. The thick solid line corresponds to the total number of events for a 3 kton detector. No oscillation effects are included.

Sc41 596.3 ms 7/2-	Sc42 681.3 ms 0+ *	Sc43 3.891 h 7/2-	Sc44 3.927 h 2+ *	Sc45 7/2- *	Sc46 83.79 d 4+ *	Sc47 3.3492 d 7/2-	Sc48 43.67 h 6+	Sc49 57.2 m 7/2-
EC	EC	EC	EC	100	$\beta^-$	$\beta^-$	$\beta^-$	$\beta^-$
Ca40 96.941	Ca41 1.03E+5 y 7/2-	Ca42 0.647	Ca43 0.135	Ca44 2.086	Ca45 162.61 d 7/2-	Ca46 0.004	Ca47 4.536 d 7/2-	Ca48 6E+18 y 0+ $\beta^- \beta^- \beta^-$ 0.137
EC	EC	0.647	0.135	2.086	$\beta^-$	0.004	$\beta^-$	$\beta^- \beta^- \beta^-$ 0.137
K39 93.2581	K40 1.277E+9 y	K41 6.7303	K42 12.360 h 2-	K43 22.3 h 3/2+	K44 22.13 m 2-	K45 17.3 m 3/2+	K46 105 s (2-)	K47 17.50 s 1/2+
3/2+	EC, $\beta^-$ 0.017	3/2+	$\beta^-$	$\beta^-$	$\beta^-$	$\beta^-$	$\beta^-$	$\beta^-$
Ar38 0.063	Ar39 269 y 7/2-	Ar40 99.600	Ar41 109.34 m 7/2-	Ar42 32.9 y 0+	Ar43 5.37 m (3/2,5/2)	Ar44 11.87 m 0+	Ar45 21.48 s	Ar46 8.4 s 0+
0+	$\beta^-$	0+	$\beta^-$	$\beta^-$	$\beta^-$	$\beta^-$	$\beta^-$	$\beta^-$
0.063	$\beta^-$	99.600	$\beta^-$	$\beta^-$	$\beta^-$	$\beta^-$	$\beta^-$	$\beta^-$
Cl37 24.23	Cl38 37.24 m 2-	Cl39 55.6 m 3/2+	Cl40 35 m	Cl41 38.4 s (1/2,3/2)+	Cl42 6.8 s	Cl43 3.3 s	Cl44 434 ms	Cl45 400 ms
3/2+	2-	3/2+	$\beta^-$	$\beta^-$	$\beta^-$	$\beta^-$	$\beta^-$	$\beta^-$
24.23	$\beta^-$	$\beta^-$	$\beta^-$	$\beta^-$	$\beta^-$	$\beta^-$	$\beta^-$	$\beta^-$
S36 0.02	S37 5.05 m 7/2-	S38 170.3 m 0+	S39 11.5 s (3/2,5/2,7/2)-	S40 8.8 s 0+	S41	S42 0.56 s 0-	S43 220 ms	S44 123 ms 0+
0+	7/2-	0+	(3/2,5/2,7/2)-	0+		0-		0+
0.02	$\beta^-$	$\beta^-$	$\beta^-$	$\beta^-$		$\beta^-$	$\beta^-$	$\beta^-$
P35 47.3 s 1/2+	P36 5.6 s	P37 2.31 s	P38 0.64 s	P39 0.16 s	P40 260 ms	P41 120 ms	P42 110 ms	P43 33 ms
1/2+	5.6 s	2.31 s	0.64 s	0.16 s	260 ms	120 ms	110 ms	33 ms
$\beta^-$	$\beta^-$	$\beta^-$	$\beta^-$	$\beta^-$	$\beta^-$	$\beta^-$	$\beta^-$	$\beta^-$

## Imaging of Cosmic and Rare Underground Sign (ICARUS) :

1. Liquid Argon time projection chamber (LArTI)
2. For solar neutrino from  $^8\text{B}$
3. For SN neutrino and oscillations

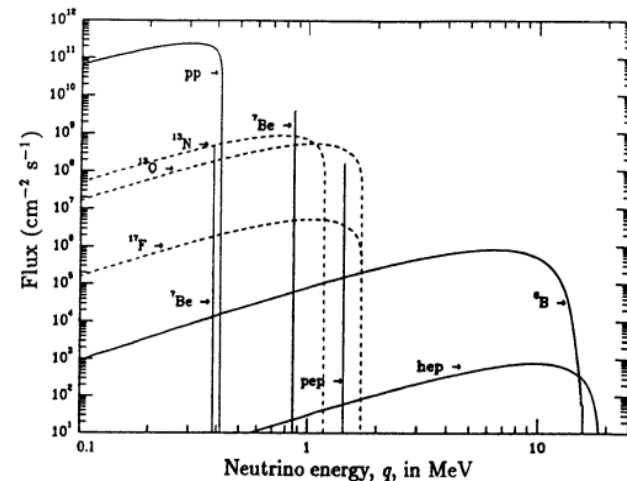
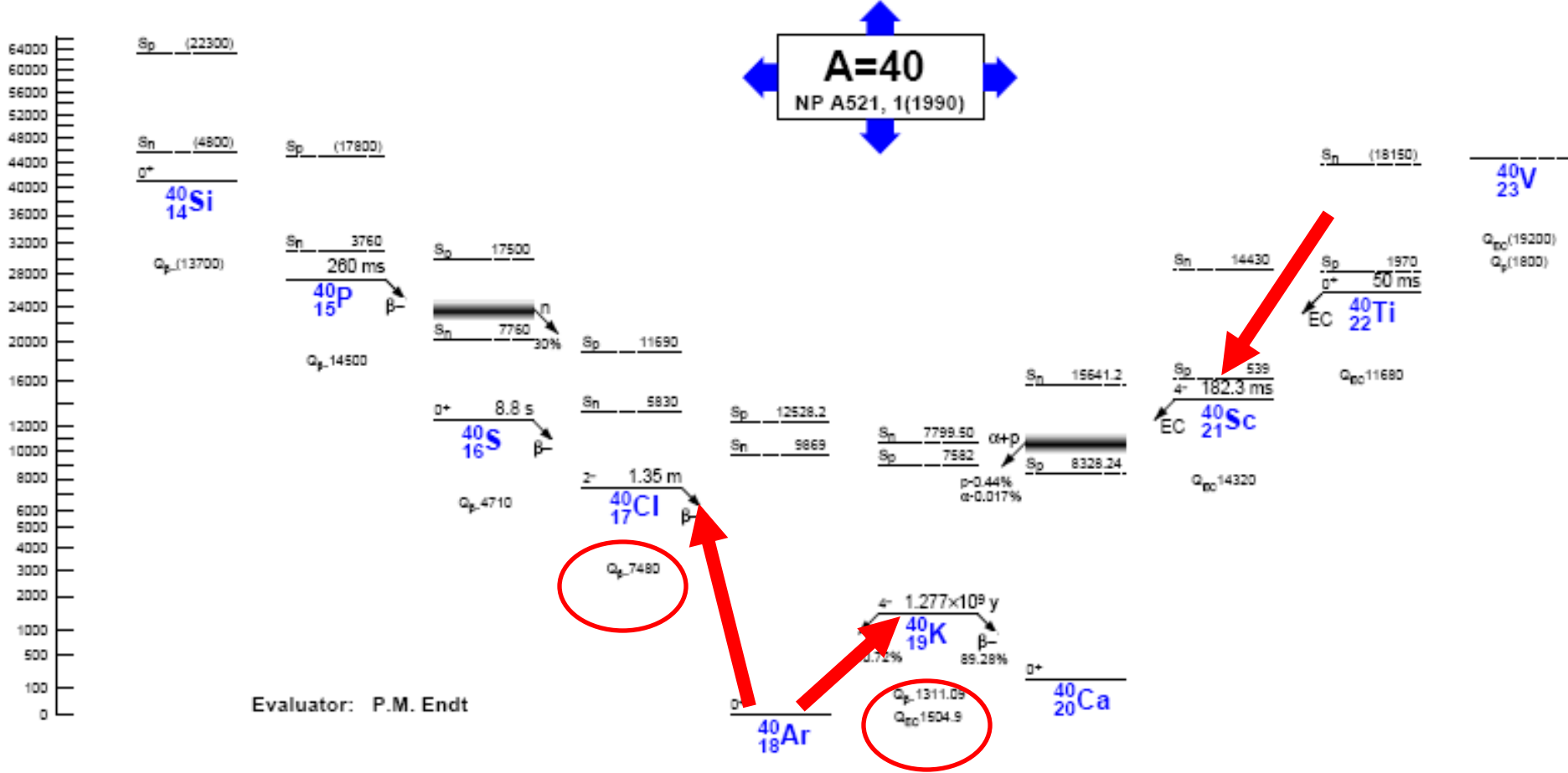
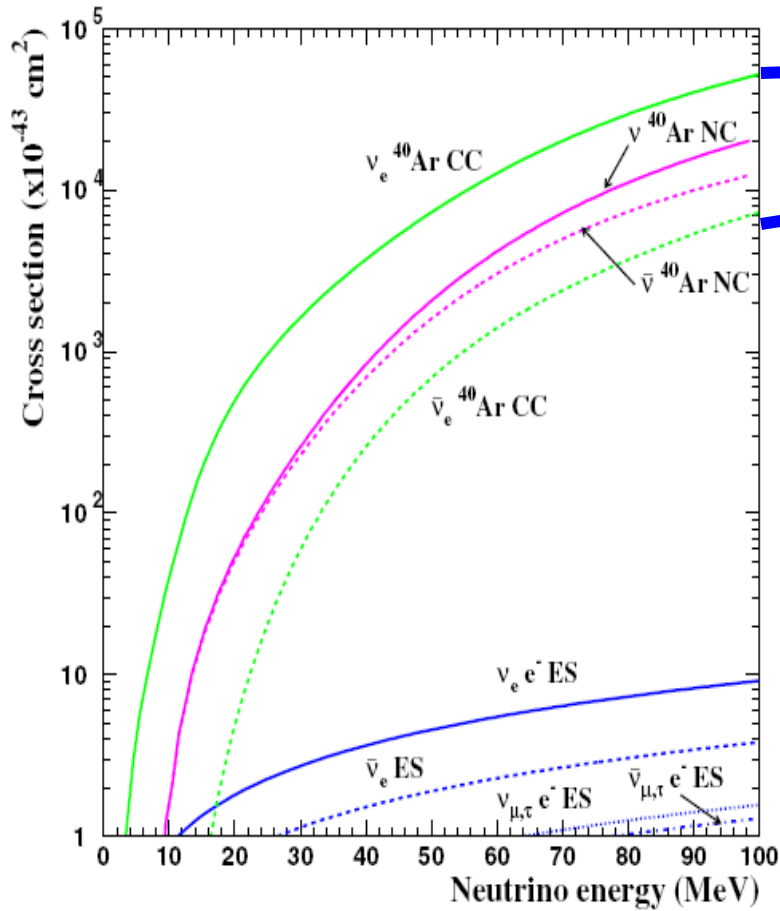


Fig. 44. Solar neutrino spectrum. Energy spectrum of solar neutrinos, as predicted by the standard solar model. Solid and dashed curves distinguish between neutrinos produced in the pp-chains and the CNO cycle, respectively. (From 49.)

# Results for 40Ar

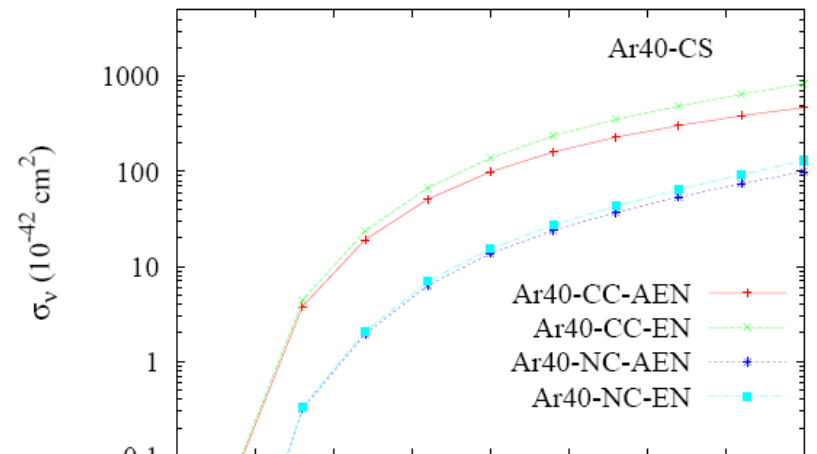
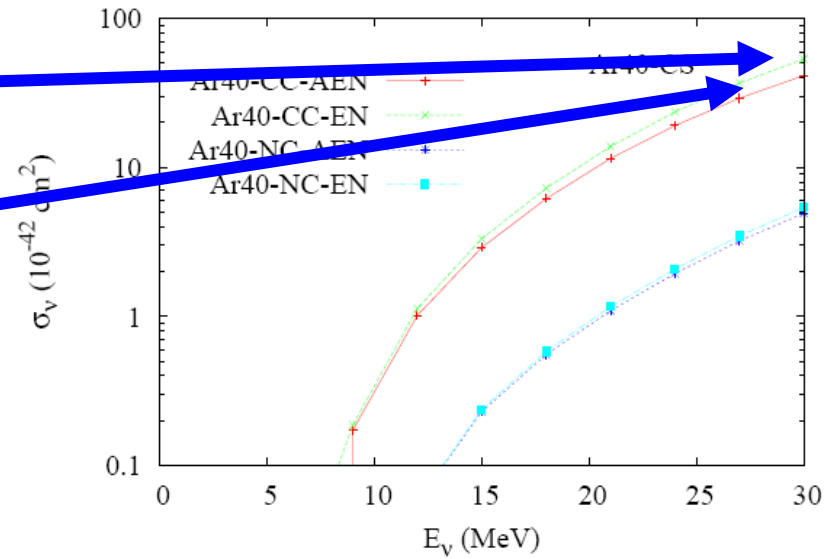




**Figure 3.** Neutrino cross sections relevant to the supernovae detection with a liquid argon TPC detector.

$$\sigma(E_\nu) = \frac{G_F^2 \cos^2 \theta_c}{\pi \hbar^4 c^3} \sum_i k_i \epsilon_i F(Z, \epsilon_i) [B_i(GT) + B_i(F)], \quad (8)$$

where  $k_i$  and  $\epsilon_i$  refer to the momentum and total energy of the outgoing electron and  $F(Z, \epsilon_i)$



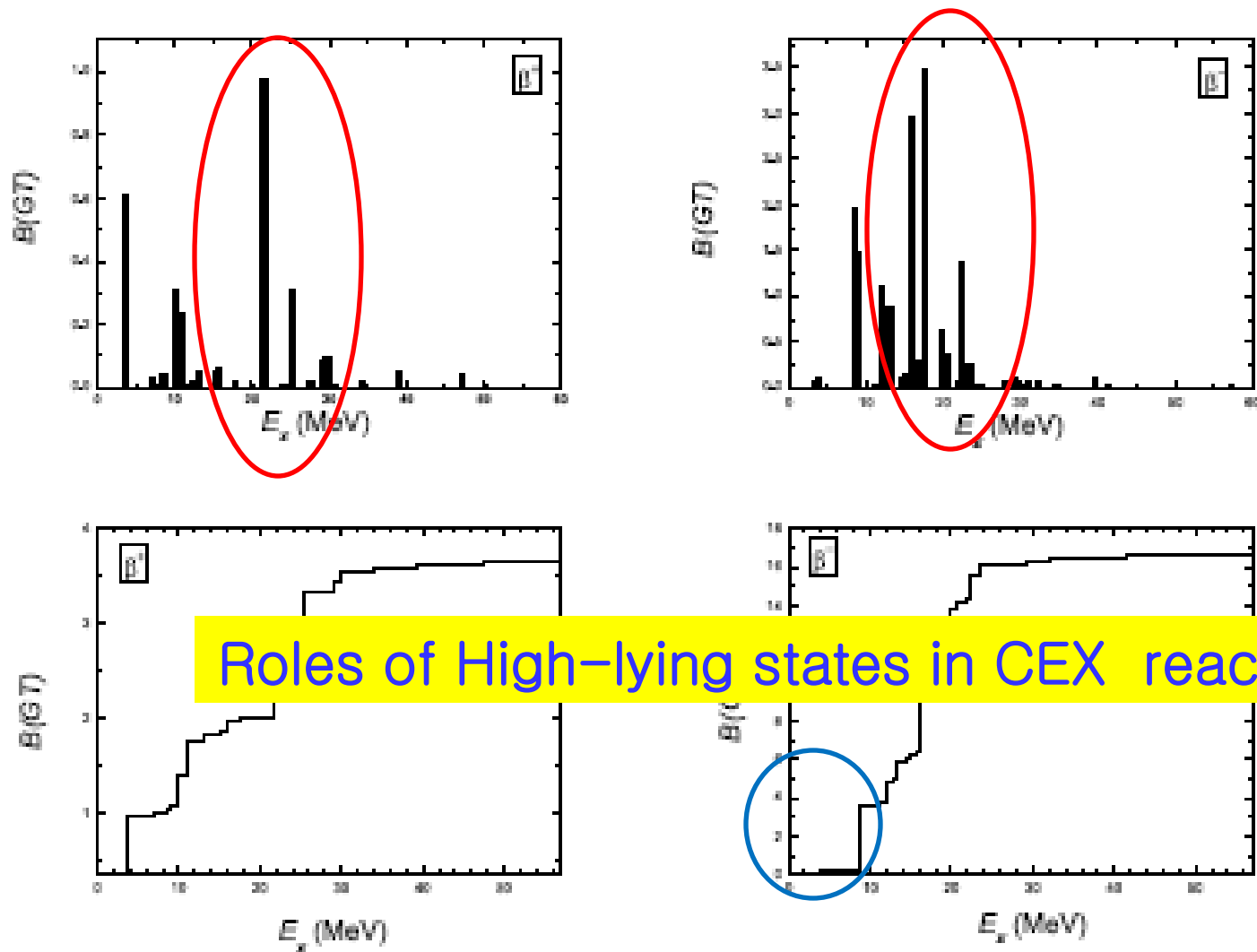


Fig. 2: The Gamow Teller strength  $\text{GT}(\pm)$  from  $^{40}\text{Ar}$  and their running sums

# Results for 92Nb

## Niobium-92

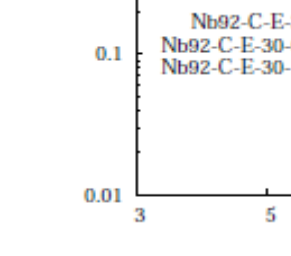
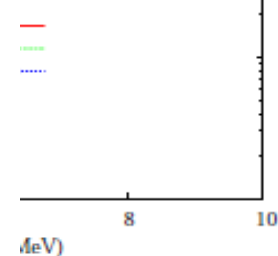
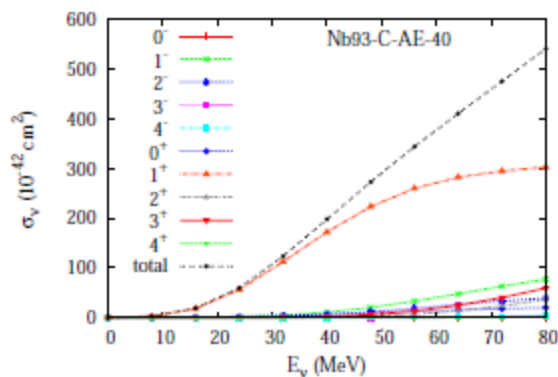
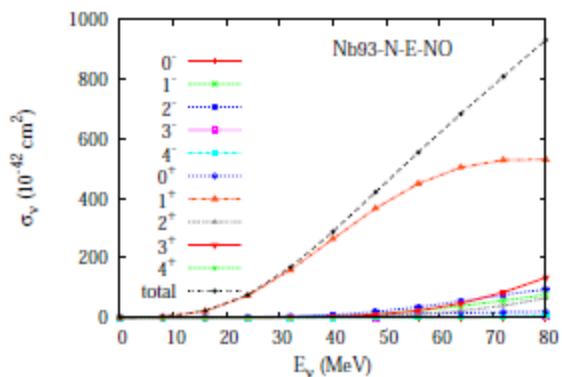
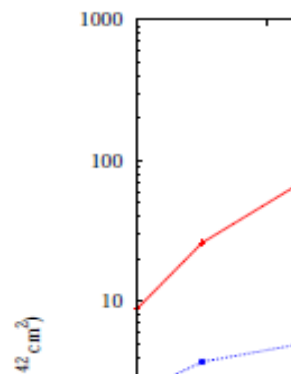
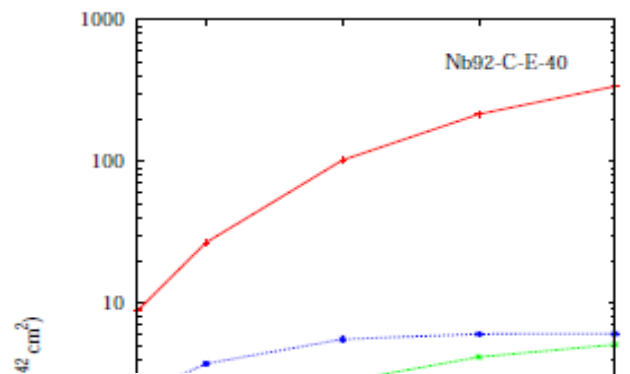
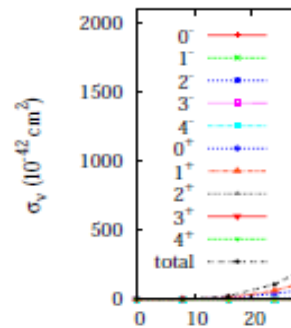
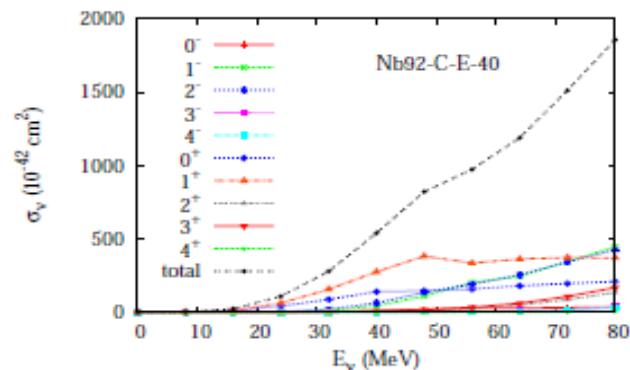
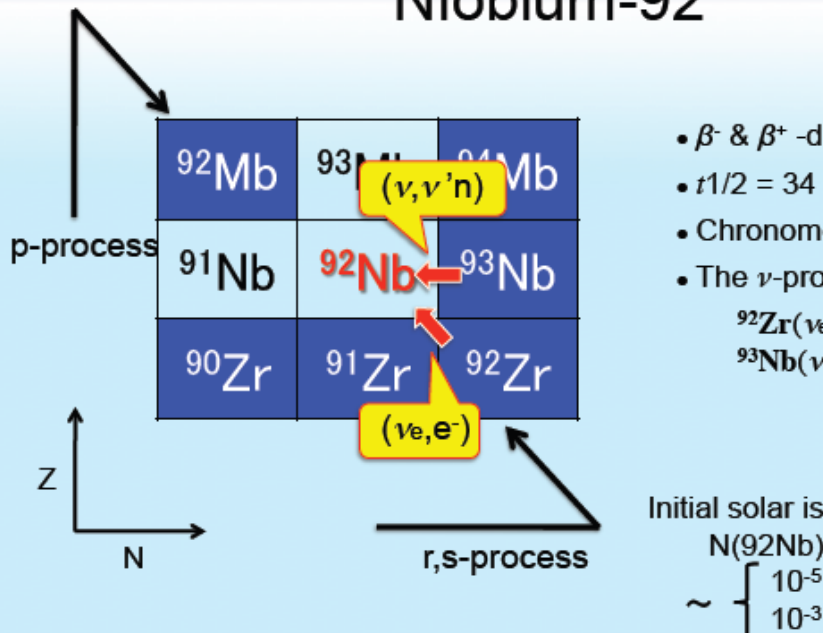


FIG. 7: Energy dependent cross sections of NC reactions for  $^{92}\text{Nb}$ ,  $^{93}\text{Nb}(\nu(\bar{\nu}), \nu'(\bar{\nu}')n)^{93}\text{Nb}$ . Left is for incident  $\nu_e$  and right is for  $\bar{\nu}_e$ .

ature dependent cross sections of CC reactions for  $^{92}\text{Nb}$ ,  $^{92}\text{Zr}(\nu_e, e^-)^{92}\text{Nb}$ . Blue and  $(\nu_e, e^-p)^{91}\text{Zr}$  and  $^{92}\text{Zr}(\nu_e, e^-n)^{91}\text{Nb}$ .

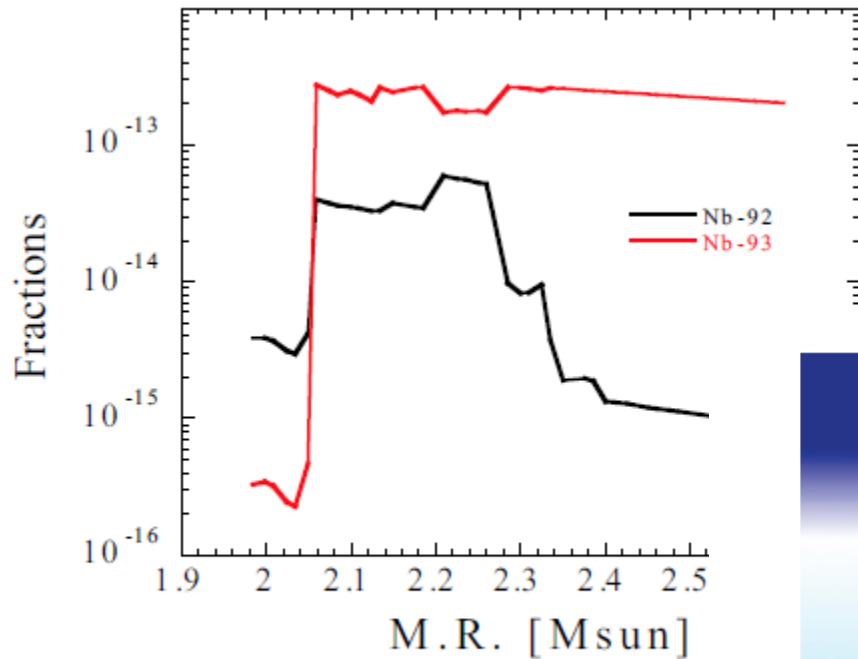


Figure 3: Calculated result of supernova neutrino

Too large ratio !

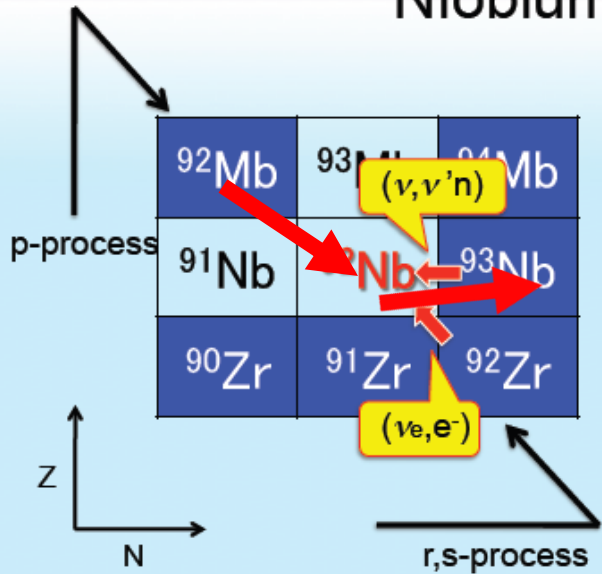
### Final mass, ratios, and observations

Total mass [Msun] in ONeMg region:		Isotopic ratios:		Solar:	
$^{92}\text{Nb}$	$= 5.4 \times 10^{-12}$	$^{92}\text{Nb}/^{93}\text{Nb}$	$= 0.21$	$\gg$	$10^{-3} - 10^{-5}$
$^{93}\text{Nb}$	$= 2.6 \times 10^{-11}$	$^{138}\text{La}/^{139}\text{La}$	$= 0.0062$	$>$	0.001
$^{138}\text{La}$	$= 8.8 \times 10^{-12}$	$^{180}\text{Ta}/^{181}\text{Ta}$	$= 0.0073$	$>$	0.0001
$^{139}\text{La}$	$= 1.4 \times 10^{-09}$				
$^{180}\text{Ta}$	$= 9.1 \times 10^{-14}$				
$^{181}\text{Ta}$	$= 1.2 \times 10^{-11}$				

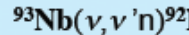
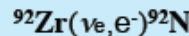
- ◆ Overproduction of  $^{138}\text{La}$  &  $^{180}\text{Ta}$   
They should be averaged over the whole.  
 $^{180}\text{Ta}$  is still too much, but a factor of 0.39 helps us.
- ◆ Overproduction of  $^{92}\text{Nb}$   
It is reasonable, because  $^{92}\text{Nb}$  is radioactive.  
The discrepancy in solar values might be caused by local formation of grains.



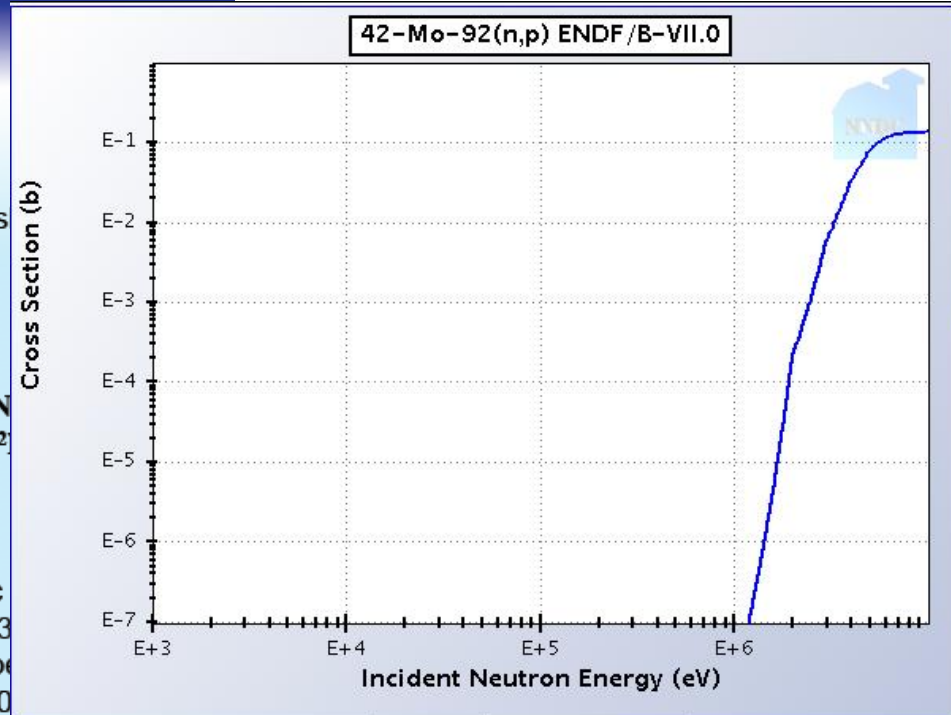
# Niobium-92



- $\beta^-$  &  $\beta^+$  -decay s
- $t_{1/2} = 34$  Myr
- Chronometer
- The  $\nu$ -process



Initial solar isotopic  
 $N(^{92}\text{Nb}) / N(^{93}\text{Nb})$   
 $\sim \begin{cases} 10^{-5} \text{ (Schoenberg)} \\ 10^{-3} \text{ (Yin+O)} \end{cases}$



Once  $^{92}\text{Nb}$  is produced by the (n,p) reaction from  $^{92}\text{Mo}$ , it is exposed simultaneously to an intense flux of neutrons and destroyed by the radiative neutron capture reaction  $^{92}\text{Nb}(n,\gamma)^{93}\text{Nb}$ . Although the (n, $\gamma$ ) cross section was not measured for the radioactive nucleus  $^{92}\text{Nb}$  ( $\tau_{1/2} = 3.47 \times 10^7 y$ ), the  $^{92}\text{Nb}(n,\gamma)^{93}\text{Nb}$  cross section is expected to be as large as those measured for stable Nb isotopes,  $\langle \sigma v \rangle / v_T = 261.3, 317.2,$  and  $402.6 \text{ mb}$  for  $^{93,94,95}\text{Nb}(n,\gamma)^{94,95,96}\text{Nb}$  reactions, respectively, at the neutron energy 30 keV [20]. These (n, $\gamma$ ) cross sections are eighteen orders of magnitude larger than the  $^{92}\text{Mo}(n,p)^{92}\text{Nb}$  cross section at this energy. Therefore, the  $^{92}\text{Mo}(n,p)^{92}\text{Nb}$  reaction should not contribute much

# Summary

- **Quasi particle RPA** with np pairing was successfully applied to the beta and double beta decays.
- The ambiguities from the nuclear structure should be pinned down for more accurate information in the astronomical data.
- ★ Results for neutrino nucleus interactions ( $^{12}\text{C}$ ,  $^{56}\text{Fe}$ ,  $^{40}\text{Ar}$ ,  $^{138}\text{La}$ ,  $^{180}\text{Ta}$ ), **obtained by QRPA showed quite consistent results with available data. But, overproduction of  $^{92}\text{Nb}$  is still open problem.  $^{93}\text{Nb}$  should be understood more clearly !!!.**
- We are applying our method to the  $\nu$  processes as well as other reactions in another nuclei.
- ★ In specific, for the unstable nuclei necessary in NS, more refined theory including the deformation, **Deformed Quasi-particle RPA (DQRPA)**, is under progress.

Thanks for your attention and  
Truly thanks  
for the INT !!

neutrino reactions. For NC reaction,

$$\begin{aligned} & \langle QRPA || \hat{O}_\lambda || \omega; JM \rangle \\ &= \sum_{a\alpha' b\beta'} [\mathcal{N}_{a\alpha' b\beta'} \langle a\alpha' || \hat{O}_\lambda || b\beta' \rangle [u_{pa\alpha'} v_{pb\beta'} X_{a\alpha' b\beta'} + v_{pa\alpha'} u_{pb\beta'} Y_{a\alpha' b\beta'}] \\ & \quad - (-)^{j_a + j_b + J} \mathcal{N}_{b\beta' a\alpha'} \langle b\beta' || \hat{O}_\lambda || a\alpha' \rangle [u_{pb\beta'} v_{pa\alpha'} X_{a\alpha' b\beta'} + v_{pb\beta'} u_{pa\alpha'} Y_{a\alpha' b\beta'}]] + (p \rightarrow n), \end{aligned} \quad (15)$$

where the normalization factor is given as  $\mathcal{N}_{a\alpha' b\beta'}(J) = \sqrt{1 - \delta_{ab} \delta_{\alpha'\beta'} (-1)^{J+T} / (1 + \delta_{ab} \delta_{\alpha'\beta'})}$ . Without the np pairing correlation, this expression can be reduced to the following simple form

$$\begin{aligned} & \langle QRPA || \hat{O}_\lambda || \omega; JM \rangle \\ &= \sum_{ab} [\mathcal{N}_{apbp} \langle ap || \hat{O}_\lambda || bp \rangle [u_{pa} v_{pb} X_{apbp} + v_{pa} u_{pb} Y_{apbp}] \\ & \quad - (-)^{j_a + j_b + J} \mathcal{N}_{bpap} \langle bp || \hat{O}_\lambda || ap \rangle [u_{pb} v_{pa} X_{apbp} + v_{pb} u_{pa} Y_{apbp}]] + (p \rightarrow n), \end{aligned} \quad (16)$$

$$\langle QRPA || \hat{O}_\lambda || \omega; JM \rangle \quad (17)$$

$$= \sum_{a\alpha' b\beta'} [\mathcal{N}_{a\alpha' b\beta'} \langle a\alpha' || \hat{O}_\lambda || b\beta' \rangle [u_{pa\alpha'} v_{nb\beta'} X_{a\alpha' b\beta'} + v_{pa\alpha'} u_{nb\beta'} Y_{a\alpha' b\beta'}]].$$

This form is also easily reduced to the results by pnQRPA without pn pairing

$$\langle QRPA || \hat{O}_\lambda || \omega; JM \rangle = \sum [\mathcal{N}_{apbn} \langle ap || \hat{O}_\lambda || bn \rangle [u_{pa} v_{nb} X_{apbn} + v_{pa} u_{nb} Y_{apbn}]]. \quad (18)$$

NC reactions cannot be described by the pn QRPA, which should be performed by pp+nn+pn QRPA by following the method for EM transition !!

